Modulations in the planetary wave field induced by upward-propagating Rossby wave packets prior to stratospheric sudden warming events: A case study

Kazuaki NISHII*, Hisashi NAKAMURA and Takafumi Miyasaka

Department of Earth and Planetary Science, Graduate School of Science, The University of Tokyo, Tokyo, 113-0033 Japan.

Abstract: A diagnostic framework is introduced in which anomalous zonally-averaged Rossby wave-activity injection into the stratosphere is decomposed into a contribution solely from zonally-confined upward-propagating Rossby wave packets and another from interaction of the wave packets with the climatological stratospheric planetary waves. To pinpoint the tropospheric sources of the wave packets, a particular form of wave-activity flux is evaluated for the associated circulation anomalies. The framework is applied to reanalysis data for the period prior to a major stratospheric sudden warming (SSW) event in January 2006, which was associated with two successive events of above normal injection of wave activity from the troposphere. In the earlier event, a pair of Rossby wave packets that emanated from tropospheric anomalies over the North Pacific and over Europe enhanced the upward wave-activity injection, which was augmented further by their interaction with the climatological planetary wave. Contrastingly in the later period, a wave packet that emanated from an anticyclonic anomaly over the North Atlantic is found to be the primary contributer to the enhanced upward planetary wave-activity injection, while its interaction with the climatological planetary wave contributed negatively. The predominant importance of the sole contribution from a single wave packet is also found in a major SSW event observed in the southern hemisphere in September 2002. These results indicate that the diagnostic framework presented in the present study is a useful tool for understanding the interaction between anomalies associated with zonally-confined Rossby wave packets and climatological-mean planetary waves in the study of stratosphere-troposphere dynamical coupling. Copyright © 2008 Royal Meteorological Society

KEY WORDS   Wave-activity flux, Blocking, Low-frequency variability

Received   ; Revised   ; Accepted

1 Introduction

In the boreal winter of 2005/06, the zonal-mean polar-night jet (PNJ) in the stratosphere gradually weakened from late December and then rapidly turned into easterly

*Correspondence to: Department of Earth and Planetary Science, Graduate School of Science, The University of Tokyo, Tokyo, 113-0033 Japan. E-mail: nishii@eps.s.u-tokyo.ac.jp

in late January (line (iv) in Figure 1a) associated with an major event of stratospheric sudden warming (SSW). The event was preceded by several events of upward injection of Rossby wave activity from the troposphere associated with planetary waves (line (i) in Figure 1a). Many observational and numerical studies, including a pioneering study by Matsuno (1971), pointed out that enhancement

of upward propagation of planetary waves from the troposphere is necessary for the occurrence of an SSW event. El Niño has been suggested as one of the possible external factors that increase the occurrence of SSW events (Labitzke 1982; Taguchi and Hartmann 2006). Owing to the sporadic nature of SSW, however, intraseasonal amplification of the planetary waves and associated enhancement of upward wave-activity injection may be of more direct importance than interannual variability of planetary wave activity associated, for example, with El Niño. In fact, the 2005/06 winter was not an El Niño winter but rather a La Niña winter.

The importance of tropospheric intraseasonal variability for SSW events has been presented in ensemble forecast experiments for particular events through a comparison between successful and unsuccessful ensemble members. For example, a forecast experiment by Mukougwa and Hirooka (2004) indicated that the amplification of tropospheric planetary waves was essential for an SSW event in the 1998/99 winter. On the basis of another forecast experiment, Mukougawa *et al.* (2005) pointed out that the formation of a blocking ridge over Europe was a key factor for the enhanced propagation of planetary-wave activity into the stratosphere during an SSW event in December 2001. These studies suggest that better prediction of SSW events requires deeper understanding and improved prediction skill of tropospheric intraseasonal variability and its interaction with the climatological planetary waves.

Most of the previous studies on the troposphere-stratosphere dynamical coupling via planetary-wave activity propagation, including these two mentioned above, were conducted in a conventional framework where waves are regarded as instantaneous departures from the zonally symmetric state for a particular latitude and they are decomposed into the zonal harmonics. Recently, there are some studies conducted in another framework where local anomalies defined as departures from a three-dimensional time-mean flow are regarded as being associated with zonally-confined wave packets. For example, Nakamura and Honda (2002) showed that the late-winter stratospheric planetary-wave field tends to be modulated significantly by interaction between the climatological planetary wave and a Rossby wave packet propagating upward from the anomalous surface Icelandic low. Nishii and Nakamura (2004a) found that lower-stratospheric intraseasonal fluctuations observed in the southern hemisphere during late winter and early spring of 1997 were often associated with zonally-confined Rossby wave packets that had originated from quasi-stationary tropospheric circulation anomalies. Nishii and Nakamura (2004b) showed that a major SSW event observed in September 2002 for the first time in the southern hemisphere followed intraseasonal amplification of a planetary-scale Rossby wave train in the stratosphere that had propagated from a tropospheric blocking flow configuration over the South Atlantic. By virtue of the particular framework adopted, these three studies have successfully pinpointed tropospheric sources of Rossby wave packets that led to the amplification of the stratospheric planetary waves.

In this study, we adopt the same framework as in Nakamura and Honda (2002) and Nishii and Nakamura (2004a, b) to analyze propagation of zonally-confined Rossby wave packets into the stratosphere in relation to tropospheric circulation anomalies during the 2005/06 winter prior to the major SSW event. Particular emphasis is placed on the upward propagating wave packets and their tropospheric wave sources. We also analyze modifications in the upward propagation of the planetary wave activity in the presence of those wave packets. We discuss

Q. J. R. Meteorol. Soc. **00**: 1–14 (2008)

DOI: 10.1002/qj

how those modifications are manifested as the amplification or weakening of the individual zonal harmonics in connection with the conventional framework in study of troposphere-stratosphere dynamical linkage. It is shown that while wave-packet propagation into the stratosphere by itself should enhance the entire upward wave-activity injection, the modifications of the climatological planetary waves by Rossby wave packets do not necessarily contribute positively to the entire upward wave-activity injection, but rather negatively in some occasions. To demonstrate the usefulness of our framework, the same diagnosis was applied to a major SSW event over Antarctica in 2002, which led to the breakdown of the ozone hole.

2 Data and diagnostic methods

In this study, we use a reanalysis data set produced by the U.S. National Centers for Environmental Prediction (NCEP) and the U.S. National Center for Atmospheric Research (NCAR) (Kalnay *et al.* 1996). The 6-hourly global atmospheric data have been provided on a regular $2.5° \times 2.5°$ latitude-longitude grid at the 17 standard pressure levels from 1000 hPa up to 10 hPa. Daily climatological-mean fields of individual variables have been constructed for the period from 1979 to 2003 based on 31-day running mean fields[†], and instantaneous anomalies are defined locally as departures of the daily fields from the daily climatology for a particular calendar day. The following results obtained from the NCEP/NCAR reanalysis data set are found consistent with those from a reanalysis data set (JRA-25) produced by the Japan Meteorological Agency (JMA) and the Central Research Institute of Electric Power Industry (CRIEPI) (Onogi et al. 2007).

In this study, the net feedback forcing from synoptic-scale transient eddies migrating along tropospheric storm tracks has been evaluated locally as the 250-hPa geopotential height tendency (Lau and Holopainen 1984):

$$\left(\nabla^2 + f^2 \frac{\partial}{\partial p}(\frac{1}{S}\frac{\partial}{\partial p}) \right) \frac{\partial \bar{Z}}{\partial t}$$
$$= -\frac{f}{g}\nabla \bullet \overline{(v'\zeta')} + \frac{f^2}{g}\frac{\partial}{\partial p}\left(\frac{\nabla \bullet \overline{(v'\theta')}}{-(\partial\Theta/\partial p)} \right), \quad (1)$$

where f denotes the Coriolis parameter, S the static stability parameter, $\partial\bar{Z}/\partial t$ the low-frequency height tendency, v' perturbation wind velocity, ζ' perturbation vorticity, θ' perturbation potential temperature, and Θ potential temperature of the background state. In Equation (1), primes signify the eddy-associated perturbations that have been extracted through 8-day high-pass filtering, and smoothing by 8-day low-pass filtering is denoted by an over-bar. The fluxes based on the 8-day high-pass-filtered data have been exposed to the low-pass filtering so as to represent feedback forcing independent of the phase of individual eddy components. It should be noted that Equation (1) is based on the linearized potential vorticity equation and $\partial\bar{Z}/\partial t$ thus evaluated includes the implicit effect of ageostrophic secondary circulations. It should also be noted that only the anomaly component of $\partial\bar{Z}/\partial t$ can contribute to time evolution of quasi-stationary circulation anomalies.

In order to represent three-dimensional propagation of a quasi-stationary Rossby wave packet in zonally-inhomogeneous westerlies, a particular form of wave-activity flux formulated by Takaya and Nakamura (2001; hereafter referred to as TN01) is used. The flux is, in theory, independent of wave phase and parallel to the local three-dimensional group velocity. In this study, the daily climatological-mean state is regarded as the basic state in which quasi-stationary Rossby waves are embedded, and

---

[†] The field was 31-day moving averaged to obtain smooth evolution of the circulation with seasonal time scale. The 25-year period is not long enough to remove day to day fluctuations from the climatology based on unfiltered daily fields for each calendar day.

5- or 10-day averaged anomalies are regarded as wave-associated fluctuations.

Although zonally-confined Rossby wave packets can be well depicted by the flux of TN01, the westerly deceleration during an SSW event is caused by upward wave-activity propagation associated not only with those Rossby-wave packets but also with the climatological planetary waves. This total upward wave-activity propagation[‡], after averaged zonally, can be represented by the vertical component of the conventional Eliassen-Palm (E-P) flux (Andrews and McIntyre 1976), which is proportional to meridional eddy heat flux across a latitudinal circle. The flux may be decomposed as

$$[V^*T^*] = [Vc^*Tc^*] + [Vc^*Ta^* + Va^*Tc^*] + [Va^*Ta^*],$$
$$\text{(2)}$$

where V and T denote the meridional wind velocity and temperature, respectively, square brackets and asterisks signify zonal averaging and deviations from the zonal mean (i.e., eddies), respectively, and the subscripts c and a denote the climatological mean and deviations from it (i.e., anomalies), respectively. The first and fourth terms on the right hand side of Equation (2) represent heat fluxes due solely to the climatological planetary waves and solely to anomalies associated with Rossby wave packets, respectively. The latter corresponds to the vertical component of TN01's flux, representing vertical wave-packet propagation. When combined, the second and third terms represent interaction between the climatological planetary waves and these wave-associated anomalies, or the particular modulating effect on the climatological planetary waves by Rossby wave-packet propagation as discussed in Nakamura and Honda (2002). The sum of

the second, third and fourth terms represents the entire modulations of the planetary waves.

Time series of the individual terms in Equation (2) at the 100-hPa level evaluated daily as average between 50°N and 80°N are presented in Figure 1b, in order to depict the upward wave-activity injection into the stratosphere. The climatological-mean and anomaly components of the flux may be expressed as

$$[V^*T^*]c = [Vc^*Tc^*] + [Va^*Ta^*]c,$$
$$\text{(3a)}$$

and

$$[V^*T^*]a = [Vc^*Ta^* + Va^*Tc^*] + [Va^*Ta^*]a,$$
$$\text{(3b)}$$

respectively. The daily value of $[Va^*Ta^*]$ tends to be positive at the 100-hPa level, and so does its climatology ($[Va^*Ta^*]c$). This is because localized upward wave-activity injection occurred spontaneously over the 25-year period, but not in a manner synchronized with the seasonal cycle, associated, for example, with blocking formation. It should be noted that $[Va^*Ta^*]c$ and $[Vc^*Tc^*]$ in Equation (3a) contributes only to the climatological seasonal march in the stratospheric zonal-mean zonal wind, and only the anomalous flux component expressed by Equation (3b) can contribute to the acceleration of zonal-mean zonal wind *anomalies*.

As represented by line (i) in Figure 1a, the total wave-activity injection into the stratosphere, which corresponds to $[V^*T^*]$, was modestly strong during the 2005/06 winter. It exceeded its climatological value $[V^*T^*]c$ (line (ii) in Figure 1a) only in the second half of November and in late December through early January. Otherwise, the injection was as strong as its climatology, and its positive anomaly never exceeded a unit standard deviation

---

[‡]Longitudinal distribution of the total upward propagation of planetary wave activity can be best represented by a wave-activity flux defined by Plumb (1985) for a zonally symmetric background flow. If averaged zonally, the flux becomes identical to the E-P flux.

(line (iii) in Figure 1a) associated with its interannual variability. In the course of the mid-stratospheric PNJ deceleration observed from late December to mid-January, the contribution from anomalies associated with Rossby wave packets $[Va^*Ta^*]$ (line (i) in Figure 1b) exceeded its climatological value $[Va^*Ta^*]c$ (line (iii) in Figure 1b). The contribution $[Va^*Ta^*]$ also exceeded that from their interaction of these wave packets with the climatological planetary waves $[Vc^*Ta^* + Va^*Tc^*]$ (line (ii) in Figure 1b) except in early January, when the latter contribution was equally important.

3 Circulation anomalies associated with upward-propagating Rossby wave packets

As mentioned in section 1, the stratospheric circulation in the 2005/06 winter was marked by the major SSW event in late January 2006 preceded by the gradual weakening of the PNJ. The particular winter was also marked by series of extreme cold surges to Europe and the Far East (Areguez *et al.* 2006). Northern Japan suffered from heavy snowfall (Mayes 2006). The cold surges were associated with pronounced quasi-stationary anomalies in the tropospheric circulation that accompanied modulations of the planetary waves. In this section, characteristics of those circulation anomalies in the troposphere and stratosphere are discussed with particular emphasis on their properties as upward-propagating Rossby wave packets.

3.1 Late December 2005

As shown in Figure 1a, the PNJ gradually weakened from late December 2005 in the presence of the enhancing upward E-P flux from the troposphere, whose intensity reached its peak in early January 2006. Snapshots of 50-hPa geopotential height anomalies for those two periods are shown in Figure 2. In late December (Figure 2a), a pair of cyclonic and anticyclonic anomalies over the northwestern Pacific and Greenland, respectively, was associated with eastward wave-activity flux from the former to the latter. As indicated with shading in Figure 2a, the anomalous upward wave-activity flux emanated into the cyclonic anomaly from a tropospheric cyclonic anomaly that corresponds to the intensified surface Aleutian low. The corresponding 250-hPa cyclonic anomaly extended zonally almost across the Pacific basin, reaching just east of Japan (Figure 2b). Our analysis of Rossby wave source (RWS), as defined by Sardeshmukh and Hoskins (1988), indicates that anomalous cyclonic vorticity forcing over Japan was associated with upper-tropospheric anomalous convergence (not shown). Located upstream of the cyclonic vorticity anomaly, this cyclonic RWS acted as forcing of that anomaly in the presence of the climatological-mean westerlies, contributing to the maintenance of the enhanced Aleutian low. The anomalous convergence that accompanied the RWS over Japan was observed in conjunction with anomalous upper-level outflow from extremely active cumulus convection over the Philippines. The effect of the corresponding low-level anomalous divergence over Japan acted to offset the anomalous positive planetary vorticity advection by the β effect. The advection arose from enhanced northerly wind associated with a surface cold surge from the Eurasian continent that occurred to the west of the intensified Aleutian low (not shown).

As evident in a zonal section for 50°N in Figure 2c, the tropospheric cyclonic anomaly in the Aleutian region was connected to the lower-stratospheric cyclonic anomaly with their phase lines tilting westward with hight. This phase tilt and the upward wave-activity flux suggest that wave activity was injected from the troposphere into the stratosphere as a zonally-confined Rossby wave

packet. The wave activity injected into the stratosphere then propagated eastward through the PNJ, generating the pair of cyclonic and anticyclonic anomalies (Figure 2a). In doing so, it modified the lower-stratospheric planetary waves, which was manifested as the eastward shift of the stratospheric Aleutian high.

3.2   Early January 2006

In early January (Figure 2d), a cyclonic anomaly over the northern Far East and an anticyclonic anomaly over the North American continent were observed in the lower stratosphere. They accompanied horizontal wave-activity flux around their centers and upward wave-activity injection from the troposphere on their upstream sides (Figure 2d). These features suggest that those stratospheric anomalies amplified with incoming Rossby wave packets from the troposphere.

In the troposphere, the cyclonic anomaly associated with the intensified Aleutian low had persisted over the North Pacific since late December (Figure 2b), while shifting its centre into the Northeastern Pacific from the south of the Aleutian islands (Figure 2e). Over Europe, a blocking dipole that consisted of cyclonic and anticyclonic anomalies to the south and north, respectively, was decaying after its mature stage at the end of December (Figure 2b), while emitting wave activity downstream (Figure 2e). As illustrated in a zonal cross section for 50°N in Figure 2f, the tropospheric anomalies associated with the anomalous Aleutian low and the blocking dipole were located upstream of the regions of the upward wave-activity injection into the stratosphere, indicating that they acted as the sources of Rossby wave packets propagating into the stratosphere. Specifically, a pair of the cyclonic anomaly at the tropopause level around 150°W over the Northeastern Pacific and the anticyclonic anomaly in the lower stratosphere around 100°W exhibited a wave-packet

structure with phase lines tilting westward with height. A similar vertical structure but with the opposite signs is found over the Eurasian continent (30°-120°E).

Figure 1b (line (i)) shows that a substantial fraction of the enhanced upward E-P flux during this period was due to a direct contribution from these upward wave packets. A comparably large contribution arose also from their interaction with the climatological planetary waves (line (ii) in Figure 1b), which will be discussed in Section 4b.

3.3   Mid-January 2006

In mid-January, just before the zonal-mean PNJ turning into easterly, the upward E-P flux slightly exceeded its climatological strength (Figure 1a). The flux was contributed to mostly by wavy anomalies themselves (line (i) in Figure 1b), which was counteracted by a contribution through their interaction with the climatological planetary waves (line (ii) in Figure 1b). As shown in Figure 3, the enhancement of the E-P flux arose mainly from strong upward propagation of a wave packet that emanated from a tropospheric anticyclonic anomaly observed over the North Atlantic and a cyclonic anomaly upstream (Figure 3b). The anticyclonic anomaly was deep, extending into the stratosphere with a slight westward tilt of its axis (Figure 3c). In the mid-stratosphere above the 50-hPa level, the anticyclonic anomaly and cyclonic anomaly downstream constituted a wave packet, accompanying prominent upward wave-activity flux between them (Figure 3c). As the cyclonic anomaly amplifies with height, the pair of the cyclonic anomaly and the anticyclonic anomaly upstream becomes the dominant feature in the mid-stratospheric anomaly field (Figure 3a).

A zonal section for 50°N in Figure 3c indicates that the tropospheric anticyclonic anomaly over the North

Q. J. R. Meteorol. Soc. **00**: 1–14 (2008)

DOI: 10.1002/qj

Atlantic and the cyclonic anomaly over the Rockies, recognized as the source of the aforementioned upward-propagating wave packet, developed in conjunction with quasi-stationary wave-like disturbances observed from the Pacific into the Atlantic across North America (Figure 3b). In addition, anomalous activity of migratory synoptic-scale transient eddies also contributed to the development of the anomalies. As shown in Figure 4a, the anomalous feedback forcing at the 250-hPa level evaluated through Equation (1) was generally anticyclonic over the North-eastern Atlantic (as strong as 100m per day in 250-hPa height tendency) and cyclonic over northwestern America (as strong as 60m per day), both of which acted to reinforce the quasi-stationary circulation anomalies effectively. This amplification of transient eddies were associated with their downstream development (Chang 1993) from the Pacific that started around 11 January (not shown).

3.4   Late January 2006

In late January, when the zonal-mean PNJ turned into easterly, the upward E-P flux into the stratosphere again slightly exceeded its climatological strength (Figure 1a). Since the circulation field in the troposphere and lower stratosphere did not change substantially during this period, the following analysis is based on 10-day mean fields for 21-30 January, as shown in Figure 5. In association with the SSW event, the Arctic stratosphere was covered entirely by an anticyclonic anomaly (Figure 5a), with their slight elongation toward Canada. The horizontal wave-activity flux emanated from that anticyclonic anomaly to a cyclonic anomaly over Europe. A zonal section for 62.5 °N in Figure 5c reveals some features that characterize upward-propagating wave-packet signatures across the tropopause over the Pacific/North American (180°W ∼ 60°W) and European sectors (30°W ∼

30°E). The wave activity was injected into those stratospheric anomalies from tropospheric wave sources that appear to be a pair of a cyclonic anomaly over Alaska and an anticyclonic anomaly over the subpolar North Atlantic (Figure 5b). The latter corresponds to a blocking high. It developed under the locally-acting feedback forcing from transient eddies, which was modestly strong (20m per day) if measured by 250-hPa height tendency (Figure 4b), and also under incoming Rossby wave activity across the Atlantic (Figure 5b). The cyclonic anomaly developed over Alaska in association with injection of Rossby wave activity from an anticyclonic anomaly over the North Pacific (Figure 5b), without any significant local feedback forcing from transient eddies (Figure 4b).

3.5   Upward wave-activity propagation and a local wave-guide structure

In this section, we have identified events of localized upward wave-activity injection into the stratosphere. However, it remains unresolved why the injection occurred in the particular regions mentioned above. To discuss the wave propagation in connection with the zonally-asymmetric climatological-mean flow, we locally evaluated the total wavenumber (κ_s) for stationary Rossby waves based on the zonally-asymmetric climatological-mean field, following Nishii and Nakamura (2004). In theory, a wave packet tends to be refracted toward local maxima of κ_s (Karoly and Hoskins 1982). Thus a local domain of κ_s maxima is favorable for wave propagation, corresponding to a local waveguide.

Figure 6 shows meridional cross sections of κ_s averaged over the individual longitudinal sectors where our analysis in this section has revealed strong upward wave-activity injection. Most of the sections in Figure 6 indicate strong upward wave-activity flux through or in the vicinities of κ_s maxima (lightly shaded in Figure 6) that extend

upward from the bottom of the stratosphere between 50
°N and 60 °N. Each of them corresponds to a vertically
extending waveguide structure associated with meridional
curvatures of the PNJ[§]. However, an exception is the situation observed in early January over the Northeastern
Pacific, where no well-defined vertical waveguide structure is analyzed in the cross section in Figure 6c. Nevertheless, strong upward wave-activity propagation occurred
between 50 °N and 70 °N with notable poleward component towards the core of the stratospheric PNJ as if a
Rossby wave packet had avoided a midlatitude domain
(heavy shaded in Figure 6) of imaginary κ_s.

4 Modulations of climatological planetary waves through their interaction with upward-propagating Rossby wave packets

As shown with line (i) in Figure 1b, enhancement of wave-activity injection into the stratosphere as represented by
the E-P flux diagnosis in late December 2005 through
late January 2006 arose mainly from a contribution due
solely to zonally-confined Rossby wave packets, as represented by the term $[Va^*Ta^*]$ in Equation (2). As was
pointed out in section 2, the peak of the upward E-P flux
(or poleward eddy heat flux) in early January 2006 was
also due to a large contribution from interaction between
the climatological planetary waves and anomalies associated with Rossby wave packets, as represented by the
term $[Vc^*Ta^* + Va^*Tc^*]$ in Equation (2) and shown in
Figure 1b with line (ii). On the contrary, the interaction
term was negative just before the PNJ turning into easterly
in mid-January. In this section modulations of the entire
planetary waves by the Rossby wave packets observed in
January were discussed mainly through an evaluation of

the interaction term in Equation (2) based on temperature
and meridional wind fields shown in Figure 7. Our evaluation was performed separately for the NCEP/NCAR and
JRA-25 data sets, and the results based on the JRA-25 data
are put in brackets into Tables I and II. Since the results
based on the two data sets are almost identical, in the following we present figures based on the NCEP/NCAR data
set.

4.1 Early January 2006

In early January, 100-hPa zonally-averaged poleward
eddy heat flux $[V^*T^*]$ between 50°N and 80°N reconstructed only from the zonal wavenumber 1-3 (k=1-3)
components was 29 [K m s^{-1}] (Table I). As evident in
Figure 7a, a positive contribution came from the southerlies with relatively warm temperatures over the Bering Sea
and the northerlies with cooler temperatures over western Russia. The temperature field includes the dominant
contribution from the k=1 component. The corresponding velocity field includes a larger contribution from the
k=2 component, yielding negative correlation with temperature over the Atlantic/North American sector (Figure
7a) to reduce the heat flux associated with the k=2 component. The k=1 component thus accounts for as much as
93% (27 [K m s^{-1}]) of the heat flux associated with the
entire planetary waves (the k=1-3 components).

The decomposition of the poleward eddy heat flux at
the 100-hPa level as in Equation (2) reveals that the climatological planetary waves $[Vc^*Tc^*]$ accounts only for 31%
of the total flux (9 [K m s^{-1}] out of 29 [K m s^{-1}]; Table
I). The main contribution to this flux component came
from the southerlies with warmer temperatures over the
Bering Sea (Figure 7b), which is in good agreement with
the region of the most enhanced upward wave-activity flux
at the 150-hPa level associated with the climatological-mean stationary waves as estimated by Plumb (1985). A

[§]In Figure 6, the vertically thin domain of κ_s minima between the 200
and 150-hPa levels reflects rapid change in static stability across the
troposphere.

stronger contribution (12 [K m s^{-1}]) came from the wave-packet term ([Va^*Ta^*]), accounting for 43% of the total flux (Table I). It arose from anomalous southerlies collocated with warm anomalies over Alaska and western Canada, and anomalous northerlies with cool anomalies over western Russia (Figure 7c). These regions correspond to local maxima of the upward wave-activity flux (Figure 2d) to which the k=1 component contributed the most (Figure 7f), especially in the temperature anomalies. At the same time, the anomalous northerlies were collocated with the climatological-mean cool temperatures over western Russia (Figure 7d). The anomalous southerlies acted to offset the climatological-mean northerlies over western Canada, where the relatively warm temperatures were observed in association with the climatological planetary waves. These features are consistent with a positive contribution from an interaction term [Va^*Tc^*], which was as strong as 11 [K m s^{-1}] (accounting for 38% of the total flux (Table I)). Meanwhile, the corresponding contribution from the other interaction term [Vc^*Ta^*] is weakly negative (-2 [K m s^{-1}]), since the correlation between Vc^* and Ta^* is positive over Europe but negative over Canada (Figure 7e).

At the tropopause level, the planetary wave field in early January 2006 was dominated by the k=1 component (Figure 8a), whose amplitude was more than twice as large as that in the climatological-mean field (Table I). The anomalous k=1 component was characterized by an anticyclonic anomaly over the Atlantic and Europe and a cyclonic anomaly over the Pacific (Figure 8d). The former strengthened a climatological ridge, while the latter acted to weaken another climatological ridge over the northeastern Pacific, leading to the eastward extension of a climatological planetary-wave trough over the Far East into the North Pacific and thereby a stronger projection onto the

k=1 component. In the lower stratosphere (50 hPa), the climatological-mean Aleutian high was elongated eastward in the presence of a positive anomaly over Canada (Figure 8e), whereas over Siberia a cyclonic eddy in the climatological-mean state was strengthened with an overlapped cyclonic anomaly. The planetary-wave field thus modified by the Rossby wave packets is projected strongly onto the k=1 component (Figures 8a and 8b), which is consistent with the increased upward E-P flux associated with that component in both the troposphere and stratosphere (Table I). No substantial change was observed in amplitude and phase of the k=2 component (Table I).

The aforementioned wave structure is elucidated further in zonal cross sections in Figures 8c and 8f. The upward-propagating planetary waves with a westward phase tilt with height over Europe and Siberia (Figure 8c) can be interpreted as the intensified climatological planetary waves due to the almost in-phase superposition of the anomalies associated with the zonally-confined wave packets (Figure 8f). The stratospheric climatological-mean Aleutian high was intensified and extended eastward by the anticyclonic anomaly that is associated with the upward-propagating wave packet from the tropospheric cyclonic anomaly over the Northeastern Pacific. This particular strengthening of the climatological planetary waves is consistent with the enhanced poleward eddy heat flux due to interaction between the climatological planetary waves and the wave-packet anomalies (Table I).

4.2 Mid-January 2006

In mid-January (Table II), the term [Va^*Ta^*] evaluated at the 100-hPa level was prominent whose strength reached as much as 12 [K m s^{-1}] as the combined contribution from the k=1-3 components, while an interaction term [Vc^*Ta^*] was strongly negative (-7 [K m s^{-1}]). The former was stronger than the contribution

from the climatological planetary waves $[Vc^*Tc^*]$ (11 [K m s^{-1}]), indicating the primary importance of the wave-packet propagation in the enhanced E-P flux into the stratosphere. The climatological-mean component was almost as strong as in early January (Figures 7b and 9b). Nevertheless, the negative $[Vc^*Ta^*]$ arose from the climatological-mean southerlies overlapping cool anomalies over the subpolar Northern Atlantic. It also arose from warm anomalies over Canada that overlapped the climatological-mean northerlies (Figure 9e). These thermal anomalies and climatological-mean meridional winds are projected mostly into the k=2 component (not shown), whose contribution to $[Vc^*Ta^*]$ was negative and as much as -10 [K m s^{-1}] (Table II). The wave-packet component $[Va^*Ta^*]$, dominated by the k=2 component (8 [K m s^{-1}]) arose from high positive correlation both between anomalous southerlies and warm anomalies over Canada and between anomalous northerlies and cold anomalies over the subpolar Atlantic (Figure 9c). The two terms $[Vc^*Ta^*]$ and $[Va^*Ta^*]$ in Equation (2) thus almost canceled out one another, resulting in the reduction of the net contribution from the $k = 2$ component to $[V^*T^*]$ at the 100-hPa level. The wind anomalies associated with the wave packet weakened the meridional winds associated with the climatological planetary waves over the North American-Atlantic sector that are dominated by the $k = 2$ component. In this manner, they act to reduce a local negative contribution from the mean state to $[Vc^*Tc^*]$ (Figures 9b and c) and thereby enhance the net upward injection of wave activity in the total planetary-wave field (Figure 9a), as a contribution primarily from the $k = 1$ component (Table I).

As shown in Figures 10a and 10d, the 250-hPa climatological-mean ridge over the Atlantic was strengthened by an overlapped anticyclonic anomaly, resulting in

the amplification of the k=1 component (150m; Table II). The k=1 component amplified also in the lower stratosphere (50 hPa). In the presence of anticyclonic anomalies over Canada and over Europe, the climatological-mean anticyclone (i.e., the Aleutian high) and the cyclonic eddy over Eurasia at the 50-hPa level were elongated eastward and westward, respectively (Figures 10b and 10e), leading to the amplification of the k=1 component (320 m; Table II). These height anomalies were nearly 180° out of phase with the climatological-mean k=2 component. Specifically the overlapping of the anticyclonic anomaly over Canada with a weak climatological-mean trough led to the weakening of the k=2 component (40 m; Table II). The amplified k=1 and weakened k=2 components compared to their climatology (190 m and 130 m, respectively) are consistent with the enhanced and diminished upward E-P flux associated with the k=1 (17 K m s^{-1}) and k=2 (-1 K m s^{-1}) components, respectively (Table II).

In a zonal cross section along 50°N (Figure 10c), an upward wave-packet-like structure is evident over the Atlantic, which is nearly in quadrature with the climatological planetary waves (Figure 10f). This phase alignment resulted in virtually no (or more precisely, slightly negative) contribution to the total eddy heat flux through the interaction between the climatological planetary waves and anomalies, as presented in Table II.

4.3   An SSW event in September 2002 in the southern hemisphere

To demonstrate the usefulness of our framework based on Equation (2), the same analysis as above was applied to the period when upward wave-activity injection was enhanced markedly during a major SSW event of the southern hemisphere (SH) observed in late September 2002 (Nishii and Nakamura 2004b). The latitudinal average was taken between 50°∼ 80°S to obtain the statistics

Q. J. R. Meteorol. Soc. **00**: 1–14 (2008)

DOI: 10.1002/qj

shown in Table III. Table III indicates that total eddy heat flux $[V^*T^*]$ was 71 [K m s^{-1}], which is much greater than its counterpart of the NH event we analyzed (Tables I and II). The wave-packet component $[Va^*Ta^*]$ accounts for 74 %, a fraction much higher than its NH counterpart. Reflecting larger amplitude of the k=1 component of the climatological planetary wave in the SH (90 [m]) in the SH than in the NH (60 [m]), its contribution to $[Vc^*Tc^*]$ and $[Vc^*Ta^* + Va^*Tc^*]$ for the SH event is also greater than for the January NH event. The dominance of $[Va^*Ta^*]$ is in agreement with Nishii and Nakamura (2004b), who found the source of the amplified planetary wave during the major SH SSW event to be localized tropospheric anomaly associated with a blocking ridge over the South Atlantic. Emanating from a localized tropospheric wave source, the wave packet consisted of several zonal harmonics and thus the k=2 and 3 yielded larger contributions than the k=1 component to $[Va^*Ta^*]$. Note that estimation of the interaction terms in Equation (2) over the Antarctica exhibits non-negligible dependence of the reanalysis data.

5   Summary and Discussions

In the present study, we have analyzed events of upward propagation of Rossby wave packets from the troposphere into the stratosphere before and during a major NH SSW event in late January 2006 and just before a marked SH SSW event in September 2002. Special attention was paid not only to local tropospheric anomalies that acted as the localized sources of those zonally-confined wave packets but also to modulations of planetary waves caused by the superposition of those wave packets on the climatological planetary waves (*i.e.* interaction).

We have found that during the preconditioning stage of the NH SSW event in early January 2006, when the PNJ axis shifted poleward as discussed below, an increase in the zonally-averaged poleward eddy heat flux for 50°∼80°N was due both to a couple of upward-propagating Rossby wave packets by themselves and to their interactions with the climatological planetary wave manifested as the amplification of its k=1 component. Just before the SSW event in late January, the enhanced eddy heat flux was dominated by a contribution from another upward-propagating Rossby wave packet, which was counteracted slightly by its interaction with the climatological planetary wave. The negative contribution arose because the positions of the tropospheric anomalies associated with the wave packet relative to the climatological planetary wave pattern happened to be unfavorable for producing upward wave-activity injection. Therefore, the relative importance of the interaction effect added to the climatological planetary wave field by a localized Rossby wave packet depends on the relative position of the packet to the phase of the planetary wave.

The presence of tropospheric anticyclonic anomalies that developed over Europe in early and late January 2006 is consistent with a composite analysis for SSW events by Limpasuvan *et al.* (2004). Likewise, tropospheric cyclonic anomalies that persisted over the Northeastern Pacific and the Northwestern America throughout January 2006 are also consistent with their analysis, although the particular cyclonic anomalies we observed were shifted slightly northward relative to their counterpart. We have confirmed that those cyclonic and anticyclonic anomalies acted as the sources of the aforementioned Rossby wave packets that propagated into the stratosphere. The apparent consistency between the results obtained from our case study and the composite analysis by Limpasuvan *et al.* (2004) suggests that amplification mechanism of planetary waves during the SSW event may be typical. Further analysis is

required, though, to generalize the findings based on our particular framework.

Our analysis has been extended to a major SH SSW event observed in late September 2002. We have found that a zonally-confined Rossby wave packet by itself carried most of the wave activity into the stratosphere. Its interaction with the climatological planetary wave accounted for a much smaller fraction, but its $k=1$ component contributed significantly to larger in the SH than NH, which reflects the weaker climatological planetary waves of its $k=2$ and 3 components in the SH. Investigation is now under way through composite analysis on whether the differences in relative importance of those heat flux terms between the NH and SH observed in the two cases is typical. The difference in amplifying mechanism of planetary waves between enhanced wave-activity propagation events in which the interaction terms contribute as in the early January case and those in which contribution from interaction terms was less important as in the mid-January case is also to be investigated.

The tropospheric anomalies analyzed in the present study were not particularly strong in the NH event in January 2006. Although the upward E-P flux observed during most of our analysis period for the NH event was stronger than its NH climatology, the positive anomaly of the flux never exceeded a unit standard deviation in strength (Figure 1a). In fact, the upward E-P flux averaged both in space between 50°N and 80°N and in time from late December 2005 to late January 2006¶ was equivalent to +0.74 if normalized by the standard deviation of its interannual variability estimated from 1979/80 to 2005/06. As shown in Figure 11, however, the deceleration of the PNJ during this winter was twice as strong as the standard deviation of the interannual variability in

the Arctic PNJ acceleration/deceleration during the same period of the winter. In recognition of the proportional constant to be almost unity between the standardized PNJ acceleration/deceleration and the normalized upward E-P flux observed for the same 40-day period for every winter (Figure 11), we speculate that other factor(s) must be operative in the outstanding PNJ deceleration in the 2005/06 NH winter. One of those factors may be the easterly phase of the stratospheric quasi-biennial oscillation (QBO), in which the equatorward dispersion of planetary wave activity tends to be reduced (e.g., Labitzke 1982). Another factor may be a poleward shift of the PNJ axis before the SSW event, which has been pointed out as a pre-conditioning for an SSW event that acts to confine the upward E-P flux to the polar stratosphere (e.g., Limpasuvan *et al.* 2004). Actually in the 2005/06 winter, the stratospheric zonal-mean zonal wind at the equator was easterly with speed of about 30 [m s^{-1}], and the zonal-mean PNJ axis in early January was shifted poleward by 5° in latitude from its climatological-mean position (62.5 °N) (not shown). Furthermore, Limpasuvan *et al.* (2007) argued about a potential contribution of episodic breaking of orographically forced gravity waves to the deceleration of the PNJ, which is, however, difficult to evaluate using reanalysis data.

Analyzing an ensemble forecast product, Hirooka *et al.* (2007) have recently found a tendency that major SSW events with higher wavenumber components preceded by minor SSW events have lower predictability than those with dominant $k=1$ component preceded by no minor events. The predictability of an SSW event depends not only on such stratospheric conditions as mentioned above but also on the predictability of tropospheric anomalies that can act as the sources of upward-propagating Rossby

¶The 40-day averaged upward E-P flux is suggested by Polvani and Waugh (2004) as a good indicator for the strength of the polar vortex.

wave packets. The present study has pinpointed the tropospheric wave sources of upward-propagating wave packets and elucidated their interaction effect acting on the climatological planetary waves prior to and during the major SSW events both in January 2006 and in September 2006. It has not been well examined, however, how sensitive the predictability of a particular SSW event tends to be to the relative contribution between the interactive modulations of the planetary waves and the precursory enhancement of wave activity injection into the stratosphere. It has not been well examined, either, how predictable those tropospheric anomalies were that acted as the sources of the upward-propagating waves. We believe that the particular framework adopted in this paper for analyzing upward-propagating Rossby wave packets is useful for studying the nature of modulations in the planetary waves and that of the development of those tropospheric anomalies including their predictability, since the framework has been used for operational analysis and a number of studies on tropospheric circulation anomalies. Predictability of tropospheric anomalies as the sources of upward propagating wave packets has some implications for extended weather forecast through the downward influence of the modulated polar vortex from the stratosphere into the troposphere. In their recent study, Takaya and Nakamura (2008) have found apparent modulations of lower-stratospheric planetary waves in late autumn with zonally-confined Rossby wave train as a precursory signal of a downward developing zonally-symmetric pressure anomaly over the Arctic in winter. Further study on dynamics and predictability of stratospheric anomalies, including SSW events, is thus needed in view of localized circulation anomalies, which have been one of the main interests in study of tropospheric dynamics and medium-range forecasts.

References

Arguez A and Coauthors. 2007. State of the climate 2006. *Bull. Am. Meteorol. Soc.*, **88:** 929–932

Andrews DG, McIntyre ME. 1976. Planetary waves in horizontal and vertical shear: The generalized Eliassen-Palm relation and the mean zonal acceleration. *J. Atmos. Sci.*, **33:** 2031–2048.

Chang EKM. 1993. Downstream development of baroclinic waves as inferred from regression analysis. *J. Atmos. Sci.*, **50:** 2038–2053

Hirooka T, Ichimaru T, Mukougawa H. 2007. Predictability of stratospheric Sudden warmings as inferred from ensemble forecast data: Intercomparison of 2001/02 and 2003/04 winters. *J. Meteorol. Soc. Jpn.*, **85:** 919–925.

Kalnay ME, Kanamitsu M, Kistler R, Collins W, Deaven D, Gandin L, Iredell M, Saha S, White G, Woollen J, Zhu Y, Leetmaa A, Reynolds R, Chelliah M, Ebisuzaki W, Higgins W, Janowiak J, Mo KC, Ropelewski W, Wang J, Jenne R, Joseph D. 1996. The NCEP/NCAR 40-year reanalysis project. *Bull. Am. Meteorol. Soc.*, **77:** 437–471.

Karoly DJ, Hoskins BJ. 1982. Three dimensional propagation of planetary waves. *J. Meteorol. Soc. Jpn.*, **60:** 109–123.

Labitzke K. 1982. On the interannual variability of the middle stratosphere during the northern winters. *J. Meteorol. Soc. Jpn.*, **60:** 124–139.

Lau NC, Holopainen EO. 1984. Transient eddy forcing of the time-mean flow as identified by geopotential tendencies. *J. Atmos. Sci.*, **41:** 313–328.

Limpasuvan V, Thompson DWJ, Hartmann DL. 2004. The life cycle of the Northern Hemisphere sudden warmings. *J. Climate*, **17:** 2584–2596.

Q. J. R. Meteorol. Soc. **00**: 1–14 (2008)

DOI: 10.1002/qj

Limpasuvan V, Wu DL, Alexander MJ, Xue M, Hu M, Pawson S, Perkins JR. 2007. Stratospheric gravity wave simulation over Greenland during 24 January 2005. *J. Geophys. Res.*, **112**, D10115, DOI: 10.1029/2006JD007823

Matsuno T. 1971. Dynamical model of stratospheric sudden warming. *J. Atmos. Sci.*, **28**: 1479–1494.

Mayes J. 2006. Nearly 4 metres of snow in Japan: Weather news. *Weather*, **61**, 34, doi: 10.1256/wea.16.06.

Mukougawa H, Hirooka T. 2004. Predictability of stratospheric sudden warming: A case study for 1998/99 winter. *Mon. Weather Rev.*, **132**: 1764–1776.

Mukougawa H, Sakai H, Hirooka T. 2005. High sensitivity to the initial condition for the prediction of sudden warming. *G*eophys. Res. Lett., **32**, L17806, doi:10.1029/2005GL022909.

Nakamura H, Honda M. 2002. Interannual seesaw between the Aleutian and Icelandic lows Part III: Its influence upon the stratospheric variability. *J. Meteorol. Soc. Jpn.*, **80**: 1051–1067.

Nishii K, Nakamura H 2004a. Lower-stratospheric Rossby wave trains in the Southern Hemisphere: A case study for late winter of 1997. *Q. J. R. Meteorol. Soc.*, **130**: 325–346.

Nishii K, Nakamura H. 2004b. Tropospheric influence on the diminished Antarctic ozone hole in September 2002. *Geophys. Res. Lett.,* **31**: doi:10.1029/GL019532.

Plumb RA. 1985. On the three-dimensional propagation of stationary waves. *J. Atmos. Sci.*, **42**: 217–229.

Polvani LM, Waugh DW. 2004. Upward wave activity flux as a precursor to extreme stratospheric events and subsequent anomalous surface weather regimes. *J. Climate*, **17**: 3548–3554.

Sardeshmukh PD, Hoskins BJ. 1988. The generation of global rotational flow by steady idealized tropical divergence. *J. Atmos. Sci.*, **45**: 1228–1251.

Takaya K, and Nakamura H. 2001. A formulation of a phase-independent wave-activity flux for stationary and migratory quasi-geostrophic eddies on a zonally basic flow. *J. Atmos. Sci.*, **58**: 608–627.

Takaya K, and Nakamura H. 2008. Precursory changes in planetary wave activity for midwinter surface pressure anomalies over the Arctic. *J. Meteorol. Soc. Jpn.*, **86**: 415–427.

Taguchi M, Hartmann DL. 2006. Increased occurrence of stratospheric sudden warmings during El Niño as simulated by WACCM. *J. Climate*, **19**: 324–332.
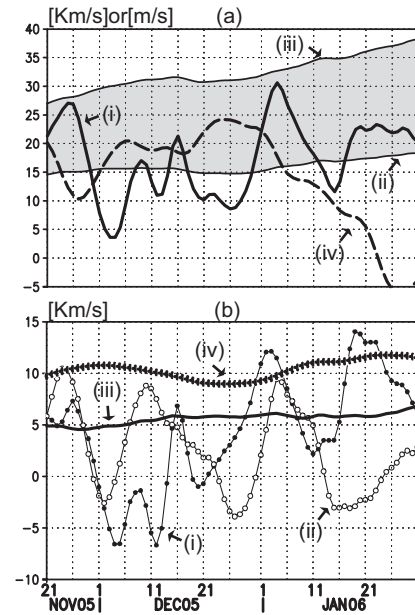
Figure 1. (a) Thick line (i): Daily time series of 100-hPa zonal-mean poleward eddy heat flux [K m s^{-1}; left axis] averaged between 50°N and 80°N. Thin line (ii): Daily climatology of the zonal-mean poleward eddy heat flux ($[Vc^*Tc^*] + [Va^*Ta^*]c$) from 1979-2003, which has been exposed to 31-day moving averaging for smoothing. Thin line (iii): Daily climatological-mean zonal-mean poleward eddy heat flux to which its unit standard deviation is added. Dashed line (iv): 20-hPa zonal-mean zonal wind [m s^{-1}; left axis] averaged between 50°N and 80°N. The heat fluxes (i), (ii) and (iii) are based on the reconstruction from contributions only from the zonal wavenumber 1-3 components at the 100-hPa level. (b) Zonal-mean poleward eddy heat fluxes [K m s^{-1}; left axis] (i: line with filled circles) due solely to anomalies ($[Va^*Ta^*]$ in Equation (2)), (ii: line with open circles) due to the interaction between the climatological-mean planetary wave and anomalies ($[Vc^*Ta^*] + [Vc^*Ta^*]$). (iii; thin line): Climatological mean of (i) ($[Va^*Ta^*]c$). (iv; line with crosses): Flux due solely to the climatological-mean planetary waves ($[Vc^*Tc^*]$). All the flux components are averaged between 50°N and 80°N and smoothed by 5-day running mean.

Table I. Contribution from the zonal harmonics (k=1, 2 and 3; and their sum) to the zonal-mean poleward heat fluxes (K m/s) at the 100-hPa level $[V^*T^*]$, the four terms as in Equation (2) that comprise $[V^*T^*]$, amplitude of 50- and 250-hPa height [m] and their climatology for the period. All based on the spatial and temporal averaging between $50^\circ \sim 80^\circ$N and for the period from 1 to 5 January 2006, respectively. Quantities are rounded off to the whole number and thus $[V^*T^*]$ in the second column is not necessarily equal to the sum of the third through fifth columns. Amplitudes of height are rounded to the nearest ten. Numbers in brackets are estimation from the JRA-25 reanalysis data, and other estimations are based on the NCEP/NCAR reanalysis data.

WN	$[V^*T^*]$	$[Vc^*Tc^*]$	$[Vc^*Ta^*]$	$[Va^*Tc^*]$	$[Va^*Ta^*]$	Z250	Zc250	Z50	Zc50
k=1-3	29 (30)	9 (10)	-4 (-1)	11 (11)	12 (10)	-	-	-	-
k=1	27 (27)	5 (6)	-2 (0)	11 (11)	13 (11)	160 (160)	60 (60)	310 (310)	150 (160)
k=2	2 (3)	4 (3)	-2 (-1)	1 (1)	-1 (-1)	120 (100)	100 (100)	130 (130)	130 (130)
k=3	0 (0)	0 (1)	0 (0)	-1 (-1)	0 (0)	30 (30)	60 (60)	30 (30)	30 (30)

Table II. The same as in Table I but based on averaging from 16 to 20 January 2006.

WN	$[V^*T^*]$	$[Vc^*Tc^*]$	$[Vc^*Ta^*]$	$[Va^*Tc^*]$	$[Va^*Ta^*]$	Z250	Zc250	Z50	Zc50
k=1-3	21 (20)	11 (11)	-7 (-8)	5 (11)	12 (11)	-	-	-	-
k=1	17 (17)	7 (6)	1 (0)	7 (7)	3 (3)	150 (140)	60 (60)	320 (320)	190 (190)
k=2	-1 (-1)	4 (4)	-10 (-10)	-3 (-3)	8 (7)	90 (90)	100 (100)	40 (30)	130 (130)
k=3	5 (5)	0 (0)	2 (2)	1 (1)	1 (1)	60 (60)	60 (60)	50 (50)	40 (40)

Table III. The same as in Table I but being based on the spatial and temporal averaging between $50^\circ \sim 80^\circ$S and for the period from 21 to 25 September 2002, respectively. The sign is reversed for each of the heat flux terms in such a way that a positive value corresponds to upwrd wave activity injection.

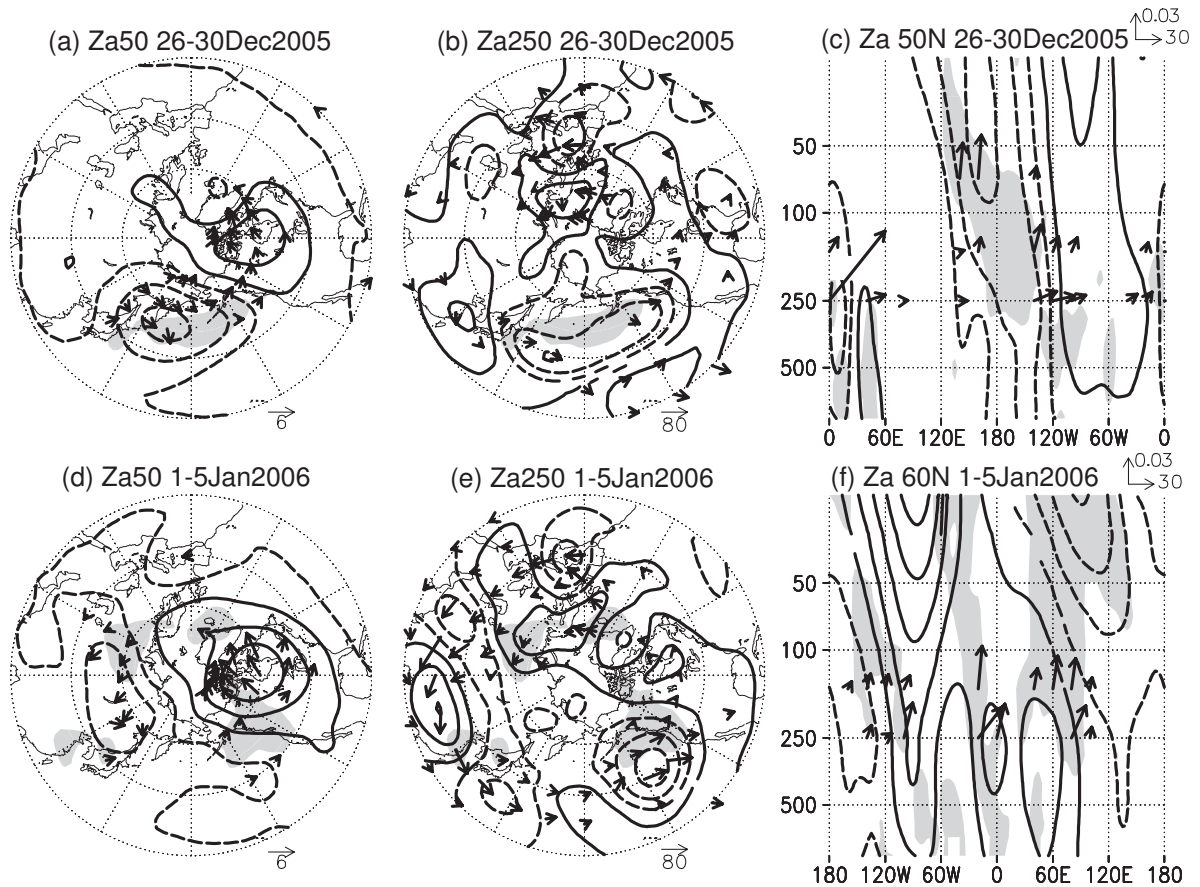| WN	$-[V^*T^*]$	$-[Vc^*Tc^*]$	$-[Vc^*Ta^*]$	$-[Va^*Tc^*]$	$-[Va^*Ta^*]$	Z250	Zc250	Z50	Zc50
k=1-3	71 (71)	9 (7)	9 (9)	0 (-2)	53 (53)	-	-	-	-
k=1	37 (36)	9 (7)	13 (9)	-4 (-7)	12 (13)	120 (120)	90 (80)	450 (460)	200 (190)
k=2	20 (22)	0 (0)	0 (4)	3 (4)	22 (22)	120 (130)	20 (20)	340 (360)	20 (30)
k=3	15 (14)	0 (0)	-4 (-4)	0 (0)	18 (18)	90 (90)	20 (20)	170 (170)	10 (20)

(a) Za50 26-30Dec2005 (b) Za250 26-30Dec2005 (c) Za 50N 26-30Dec2005

(d) Za50 1-5Jan2006 (e) Za250 1-5Jan2006 (f) Za 60N 1-5Jan2006

Figure 2. (a) 50-hPa height anomalies averaged over the period from 26 to 30 December 2005 (contoured for ±60, ±180 and ±300 m) and the horizontal component of an associated wave-activity flux (arrows). Solid and dashed lines represent anticyclonic (positive) and cyclonic (negative) anomalies, respectively. Those anomalies are multiplied by a factor $f(43°N)/f(lat)$ to mimic streamfunction-like anomalies. Scaling for the arrows [Unit: m^2 s^{-2}] is given at the lower-right corner of each panel. Shading indicates the upward component of the wave-activity flux at the 100-hPa level whose magnitude exceeds 0.02 [m^2 s^{-2}]. (b) The same as in (a) but for the 250-hPa level. (c) Zonal section for 50°N of height anomalies (contoured for ±60, ±180 m, ±300 m, ±420m and $\pm$ 540 m) and an associated wave-activity flux (arrows). Scaling for the arrows is given near the upper-right corner of the panel [Unit: m^2 s^{-2}]. Shading indicates the upward component of the wave-activity flux whose magnitude exceeds 0.2 [m^2 s^{-2}]. (d), (e), (f) As in (a), (b) and (c), respectively, but for the period from 1 to 5 January 2006.

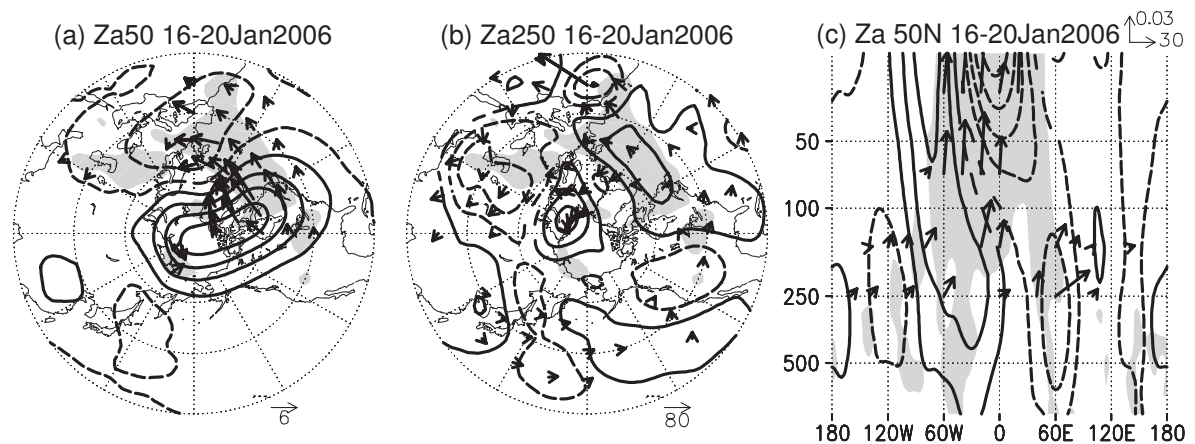## (a) Za50 16-20Jan2006 (b) Za250 16-20Jan2006 (c) Za 50N 16-20Jan2006

Figure 3. (a) (b) (c) As in Figures 2a, 2b and 2c, respectively, but for the period from 16 to 20 January 2006.
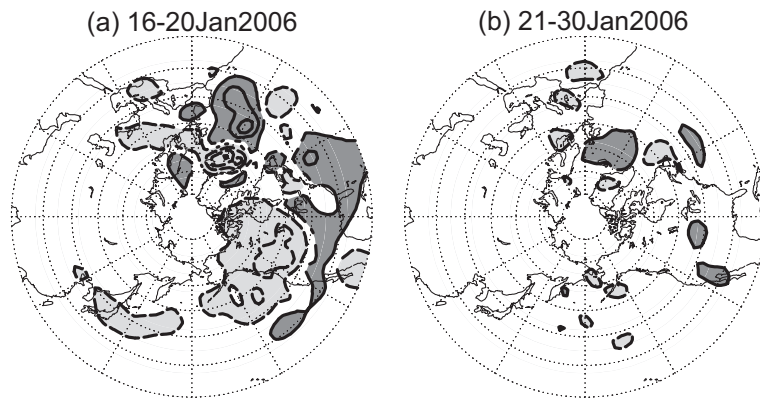
Figure 4. (a) The net anomalous feedback forcing by high-frequency transient eddies through their vorticity and heat fluxes (Equation (1)) averaged from 16 to 20 January 2006, represented as 250-hPa anomalous height tendency (contour; ±20, 60 and 100 [m day^{-1}]). Heavy and light shading denotes the height tendency exceeding 20 [m day^{-1}] in magnitude positively and negatively, respectively. (b) As in (a) but for the period from 21 to 30 January 2006.
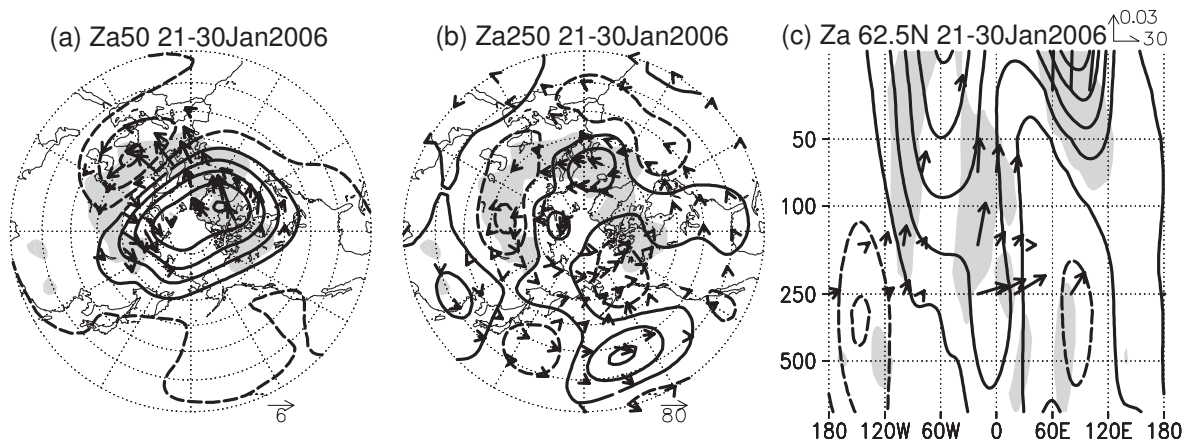

Figure 5. (a)(b)(c) As in Figures 2a, 2b and 2c, respectively but for the period from 21 to 30 January 2006. In (c), zonal cross section was constructed for 62.5°N.

Figure 6. (a) Total stationary Rossby wavenumber (κ_s) averaged zonally from 150 to 180°E based on the climatological-mean state for the period from 26 to 30 December 2005, represented as the "equivalent zonal wavenumber" (thin line) for each latitude (i.e. κ_s divided by the earth radius and cosine of the latitude). Heavy shading is applied where κ_s is imaginary and light shading where κ_s exceeds 2.5. Thick contours denote the upward wave-activity flux of 0.2 [m^2 s^{-2}] averaged for the period. Arrows indicate the meridional and vertical components of a wave-activity flux. Scaling for the arrows [Unit: m^2 s^{-2}] is given at the upper-right corner. (b) The same as in (a) but for the zonal average between 50° and 80°E for the period from 1 to 5 January 2006. (c) The same as in (a) but for the zonal average between 210° and 240°E for the period from 1 to 5 January (2006). (d) The same as in (a) but for the zonal average between 300° and 330°E for the period from 16 to 20 January 2006. (e) The same as in (a) but zonal average between 0° and 30°E for the period from 21 to 30 January (2006). (f) The same as in (a) but for the zonal average between 240° and 270°E for the period from 21 to 30 January 2006.
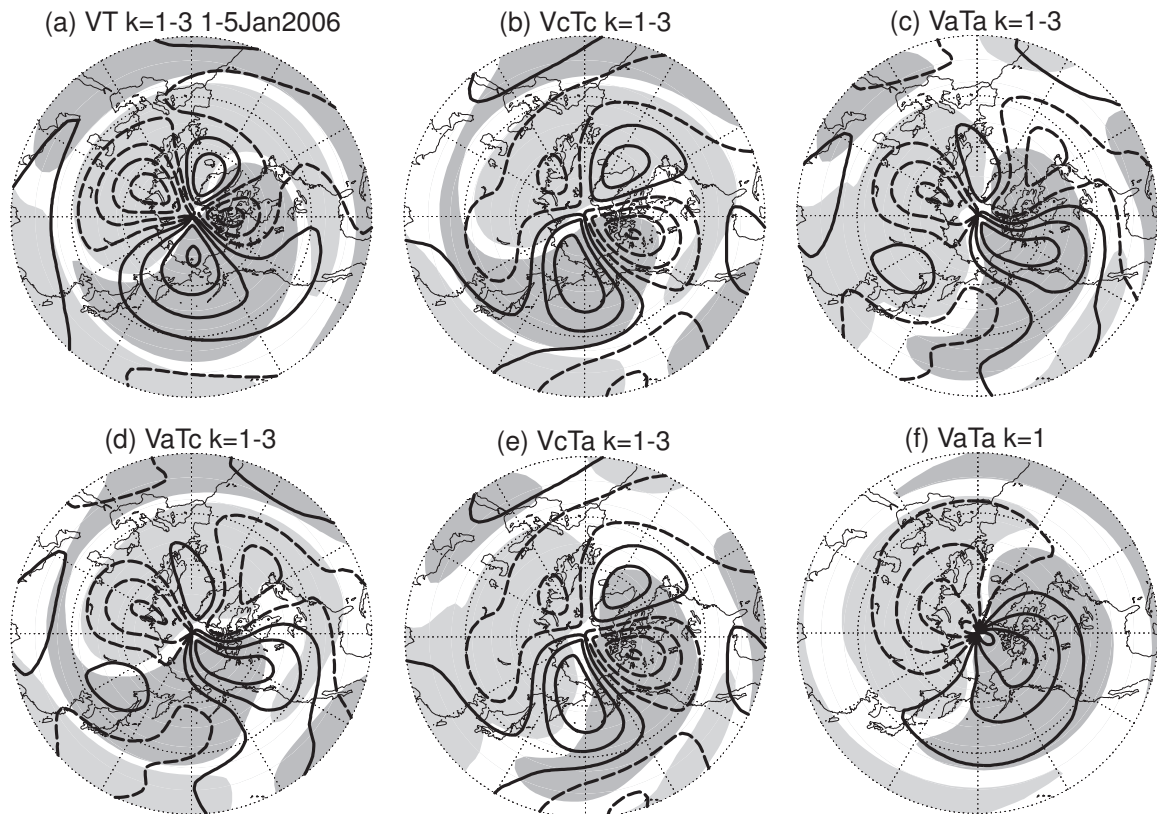
Figure 7. (a) Planetary waves in meridional wind (contoured) and temperature (shaded) fields at the 100-hPa level averaged for 1-5 January 2006, reconstructed only from the k=1-3 components. (b) As in (a) but for the climatology for 1-5 January. (c) As in (a) but for the reconstructed wind and temperature anomalies. (d) Anomalous meridional wind velocity (contoured) and climatological-mean temperature (shaded). (e) Climatological-mean temperature (contoured) and anomalous temperature (shaded) (f) As in (c) but for the anomalies associated only with k=1 component. In each of the panels, meridional wind velocity is contoured (for $\pm 2, \pm 6, \pm 10$ [m s^{-1}]; dashed for northerlies). Heavy (light) shading is applied for temperatures warmer (cooler) than the zonal mean by more than 2 K.
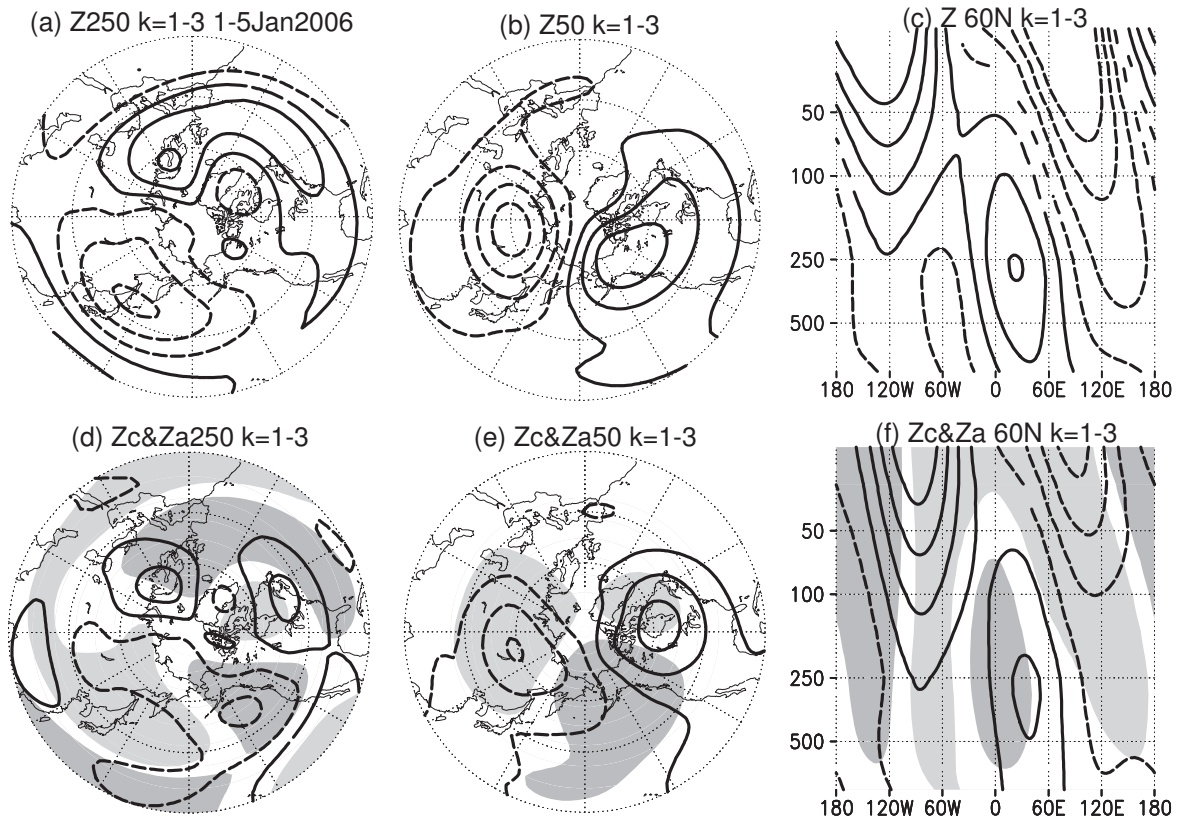
Figure 8. Planetary waves in mean geopotential height field for 1-5 January 2006 reconstructed only from the k=1-3 components. (a) Geopotential height at the 250-hPa level. (b) As in (a) but at the 50-hPa level. (c) As in (a) but for zonal cross section for 60°N. (d) As in (a) but for height anomaly (contoured) and climatology (heavy shading for 60 [m] or more and light shading for -60 [m] or less). (e) As in (d) but at the 50-hPa level. (f) As in (d) but zonal cross section for 60°N. In each of the panels, the height field has been multiplied by a factor $f(43°N)/f(lat)$ to mimic streamfunction-like anomaly. The contours are drawn for $\pm60, \pm180, \pm300$[m] and dashed for negative values.
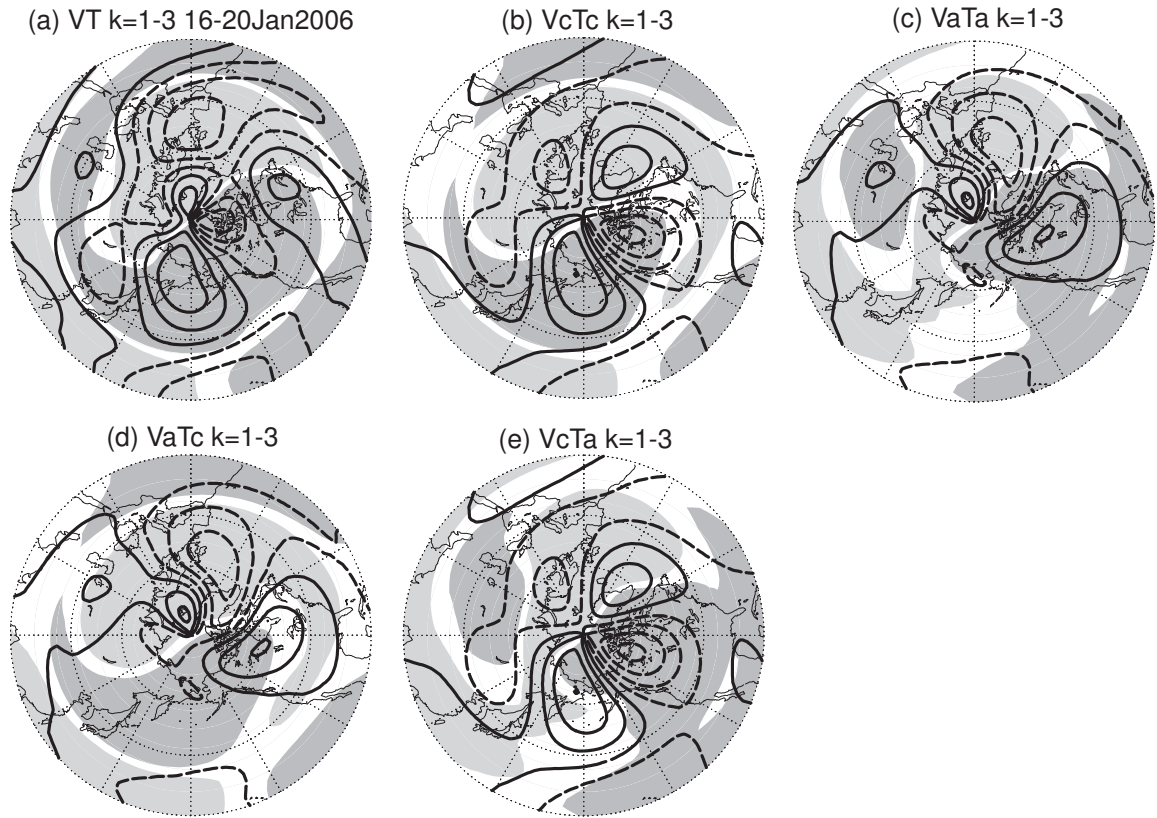
(a) VT k=1-3 16-20Jan2006

(b) VcTc k=1-3

(c) VaTa k=1-3

(d) VaTc k=1-3

(e) VcTa k=1-3

Figure 9.   Same as in Figure 7 but averaged for the period from 16 to 20 January 2006.

(a) Z250 k=1-3 16-20Jan2006

(b) Z50 k=1-3

(c) Z 50N k=1-3

(d) Zc&Za250 k=1-3

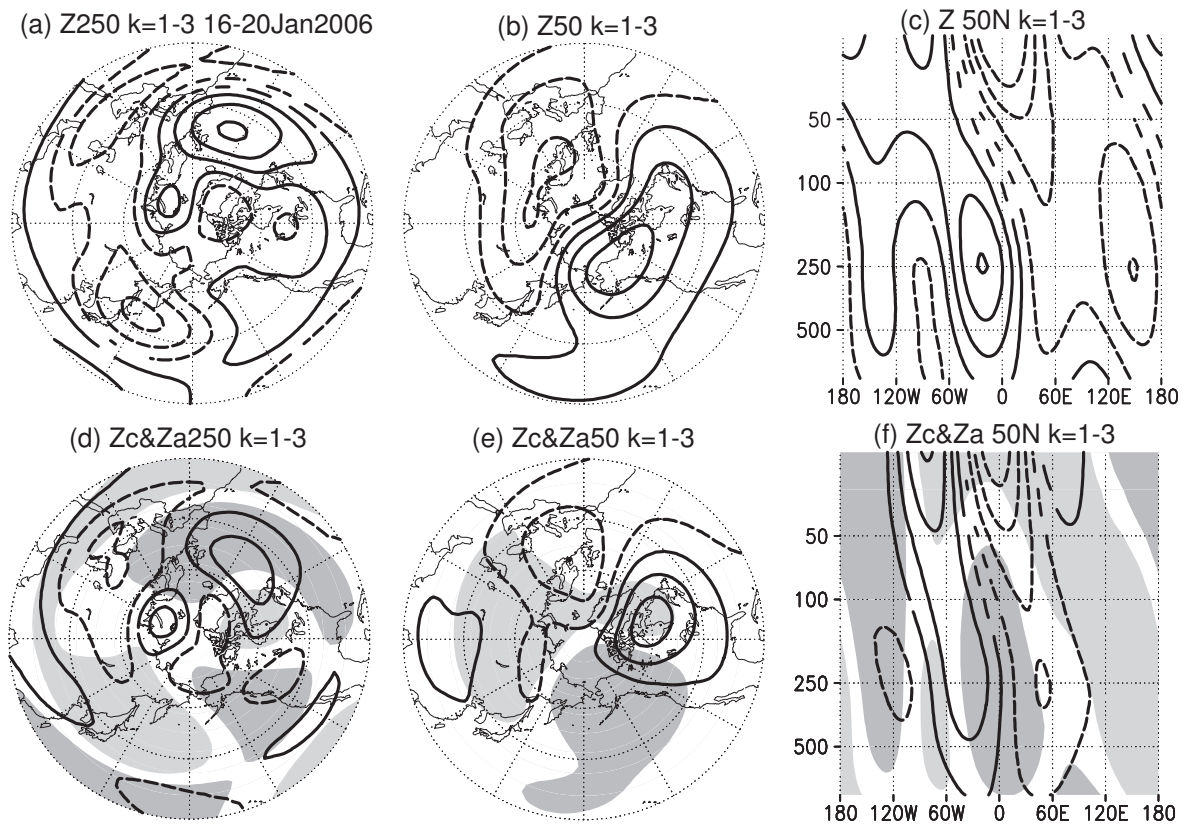(e) Zc&Za50 k=1-3

(f) Zc&Za 50N k=1-3

Figure 10.   Same as in Figure 8 but averaged for the period from 16 to 20 January 2006. Note that zonal sections in (c) and (f) are taken for 50°N.
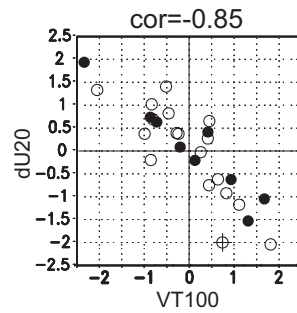
Figure 11.   A scatter diagram showing the relationship between poleward eddy heat flux averaged from 21 December to 30 January and 20-hPa zonal-mean wind tendency taken as difference between the two periods, one from 21 to 30 January of a given year and the other from 21 to 30 December of the preceding year, for individual winters from 1979/80 to 2005/06. Each of the quantities is averaged between 50 °N and 80°N and normalized with the standard deviation for its interannual variability. Their correlation coefficient is -0.85. Filled and open circles denote winters in which 30-hPa Equatorial zonal-mean zonal wind was westerly and easterly, respectively, for the period 21 December through 30 January. The 2005/06 winter is emphasized with a cross.